



# Exploring Deep Learning Architectures for RF Signal Classification

POLÁK, L.; TURÁK, S.; ŠOTNER, R.; KUFA, J.; MARŠÁLEK, R.; DHAKA, A.

35th International Conference Radioelektronika

pages: 1-6

eISBN: 979-8-3315-4447-8

eISSN: 2767-9969

DOI: https://doi.org/10.1109/RADIOELEKTRONIKA65656.2025.11008396

Accepted manuscript

©2025 IEEE. Personal use of this material is permitted. Permission from IEEE must be obtained for all other uses, in any current or future media, including reprinting/republishing this material for advertising or promotional purposes, creating new collective works, for resale or redistribution to servers or lists, or reuse of any copyrighted component of this work in other works. POLÁK, L.; TURÁK, S.; ŠOTNER, R.; KUFA, J.; MARŠÁLEK, R.; DHAKA, A. "Exploring Deep Learning Architectures for RF Signal Classification", Radioelektronika 2025. DOI: 10.1109/RADIOELEKTRONIKA65656.2025.11008396. Final version is available at <a href="https://ieeexplore.ieee.org/document/11008396">https://ieeexplore.ieee.org/document/11008396</a>

## Exploring Deep Learning Architectures for RF Signal Classification

Ladislav Polak, Samuel Turak, Roman Sotner, Jan Kufa, Roman Marsalek Brno University of Technology FEEC, Department of Radio Electronics Technicka 12, 616 00 Brno, Czech Republic samuel.turak@gmail.com, polakl@vut.cz Arvind Dhaka

Dept. of Computer and Communication Engineering

Manipal University Jaipur

Rajasthan, India

arvind.neomatrix@gmail.com

Abstract—Future 6G radio networks will heavily rely on deep learning (DL) models for both signal and data processing. DL-based solutions can be highly effective in classifying various radio frequency (RF) signals influenced by noise or intentional jamming as they are capable of recognizing patterns even under challenging conditions. This paper focuses on the classification of different RF signals using three DL-based models: CNN, GRU, and CGDNN. For this purpose, a dataset containing RF signals influenced by various impairments (e.g., I/Q-imbalance) and transmission conditions (e.g., multipath propagation) was created using MATLAB. Both the dataset and the source code have been made publicly available to support further research in this area. Preliminary results shown that the performance of DL-based approaches depends not only on the RF impairments considered but also on the preparation of the dataset.

*Index Terms*—Classification, Channel models, Dataset, Deep learning, Neural networks, RF impairments, RF signals.

#### I. INTRODUCTION

Wireless communications is one of the fastest growing fields. Recently, various mobile (such as 4G and 5G) and wireless technologies (like Wi-Fi and LoRa) have expanded the possibilities for achieving good coverage and seamless connectivity [1]–[3]. Future generations of wireless technology, often referred to collectively as 6G, present a new set of challenges for engineers. These include the need for higher data rates and spectral efficiency, improved reliability, and safer information transmission [4]. To meet these goals, unconventional approaches, such as the integration of Deep Learning (DL) architectures in signal processing and the development of future radio networks, will be required [5]–[7].

DL-based automatic modulation classification (AMC) [8] and radio frequency (RF) signal classification [9] are among the hottest topics in wireless communication, as evidenced by the growing number of studies in recent years. In [10], the Convolutional Neural Network (CNN) and Convolutional Long-Short-Term Deep Neural Network (CLDNN) with reduced number of parameters were introduced for AMC. The potential of DL-based approaches compared to conventional methods was shown [11]. Various DL-based architectures, including CNN and Recurrent Neural Networks (RNN), have been employed to propose AMC methods in [12] and [13].

Research described in this paper was financed by MEYS project LUC24141.

In both cases, the dataset was generated using GNU Radio [14]. Simulation-based results confirmed the strong performance of these DL-based architectures for AMC across different signal-to-noise ratio (SNR) levels. In [15], a Convolutional Gated Deep Neural Network (CGDNN) architecture was introduced for AMC over a Rician fading channel, with the dataset generated using MATLAB. The results demonstrated that the CGDNN performed well under various Rician K-factors.

Shi et al. [16] explored the use of CNNs for signal (modulation) classification, including scenarios with superimposed or jammed signals. Their model achieved high accuracy in classifying RF signals within unknown spectrum environments. In [17], a CNN-based framework called SigNet was proposed for radio signal classification. This framework shown good classification accuracy, even when using a very small training set. Both studies primarily used the well-known dataset [14]. Another CNN-based method for RF signal detection was presented in [18] and [19], further highlighting the capabilities of DL-based methods in this domain. Additionally, in [20], a DL-approach combining CNN and RNN architectures was tested to classify coexisting Wi-Fi, Long-Term Evolution (LTE), and 5G signals. The waveforms were generated using MATLAB, and the results showed promising accuracy for RF signal classification in various scenarios.

Contribution: This paper examines the classification accuracy of three different DL architectures, namely CNN, Gated Recurrent Unit (GRU), and CGDNN, for RF signals influenced by various imperfections. The dataset was entirely generated using highly flexible MATLAB's Wireless Waveform Generator. Unlike previous studies, this work also considers different wireless standards, such as ZigBee and Bluetooth, which have not received significant attention in earlier research. To promote reproducibility, the dataset and the source code for this simulation-based study are publicly available [21], [22].

The remainder of this paper is organized as follows. The DL-based architectures used in this work are briefly introduced in Section II. The dataset and the simulation-based study are described in Section III. The obtained results are evaluated in Section IV. This paper is concluded in Section V.

### II. DL ARCHITECTURES FOR RF SIGNAL CLASSIFICATION

In this study, three DL-based architectures, originate from works with focus on AMC, are evaluated for RF signal classification. These models were initially tested on specific RadioML datasets [14].

#### A. CNN

The used architecture of CNN model, introduced in [10], was originally applied for AMC. The input layer, see Fig. 1, accepts the input vector (I/Q-data<sup>1</sup>) one by one and its output is framed with zeros at the zero-padding layer, enabling the kernel of the following convolutional layers to access the border regions of the data. There are three convolutional 1D layers, meaning the kernel moves only across one dimension, producing only a 2D feature map (length and channel). The rectified linear activation function (ReLU) is utilized in these layers. Following each convolutional layer is max-pooling, with an additional Dropout layer to randomly omit a subset of features during training. The flatten layer convert the data dimensions into a 1D vector. The first dense layer is activated by scaled exponential linear unit function (SeLu), while the second is activated by the Softmax function, transforming the neuron weighs into 4 probabilities [22]. The setting of the CNN architecture is listed in Table I.



Fig. 1. Block scheme of the CNN model

TABLE I: Hyperparameter setting for CNN [10]

Layer	Hyperparameters	Output Shape
Input	-	$256 \times 2$
Zero padding	Padding 4	$264 \times 2$
Conv 1D	Filters = 50, Kernel Size = 8, ReLu	$257 \times 50$
Max Pooling 1D	Pool size = 2	$128 \times 50$
Conv 1D	Filters = 50, Kernel Size = 8, ReLu	121 × 50
Max Pooling 1D	Pool size = 2	$60 \times 50$
Conv 1D	Filters = 50, Kernel Size = 4, ReLu	57 × 50
Dropout	0.6	57 × 50
Max Pooling 1D	Pool size = 2	$28 \times 50$
Flatten	-	1400
Dense	70 Units, SeLu	70
Dense	4 Units, Softmax	4

#### B. GRU

The architecture of GRU (see Fig. 2), inspired by [12], includes over 1,600,000 parameters, allowing it to learn a wide range of features from the data. However, it requires significant computational resources and is susceptible to overfitting. Each GRU layer incorporates a ReLU activation function. Increasing the number of units within the GRU layers leads to higher accuracy and the model's parameter count. In this work, 50 units per layer are used to balance performance and complexity. Dropout with a rate of 0.6 was introduced after each GRU layer to mitigate overfitting.

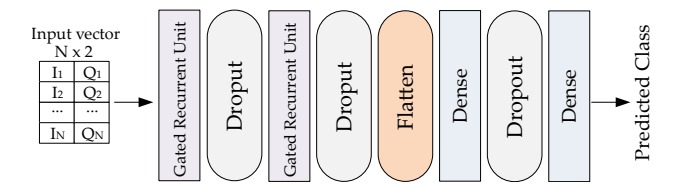


Fig. 2. Block scheme of the GRU model.

TABLE II: Hyperparameter setting for GRU [12]

Layer	Hyperparameters	Output Shape
Input	-	$256 \times 2$
GRU	Units = 50	$256 \times 50$
Dropout	0.6	$256 \times 50$
GRU	Units = 50	$256 \times 50$
Dropout	0.6	$256 \times 50$
Flatten	-	12800
Dense	128 Units, ReLu	128
Dropout	0.6	128
Dense	4 Units, Softmax	4

Similar to the CNN architecture, a flatten layer was added to convert the multidimensional data into a 1D vector. Next, a dense layer with more than 128 neurons was added, significantly contributing to the high parameter count of this model. Unlike in the CNN, the activation for this layer is ReLu. The last Dense layer follows with softmax activation. The setting of the GRU architecture is shown in Table II.

#### C. CGDNN

Two main concepts behind the CGDNN model focus on leveraging the strengths of both CNNs and RNNs [15]. The model utilizes an RNN, specifically a GRU layer, to process sequential data. Following the GRU layer, the architecture employs Convolutional 1D layers to capture additional relevant features from the sequential output. This fusion is shown in Fig. 3. The network includes standalone ReLU activation functions to introduce nonlinearity, enhancing its capacity to learn complex patterns. Batch normalization is applied after each convolutional layer to mitigate potential data distribution shifts, normalizing inputs to subsequent layers and stabilizing the learning process, which increases network efficiency. To reduce overfitting, dropout with a rate of 0.2 is employed. The CGDNN architecture also includes an Average Pooling layer after the first convolutional layer to reduce the dimensionality of the feature maps. The configuration details, including the number of filters and kernel sizes, are carefully selected to maintain a low parameter count while still meeting the design goals of the model. The setting of the CGDNN architecture is summarized in Table III.



Fig. 3. Block scheme of the CGDNN model.

 $<sup>^{1}</sup>I$  - In-Phase, Q - Quadrature

TABLE III: Hyperparameter setting for CGDNN [23]

Layer	Hyperparameters	Output Shape
Input	-	$256 \times 2$
GRU	Units = 80	$256 \times 80$
Batch Normalization	-	256 × 80
ReLu	-	256 × 80
Dropout	0.2	$256 \times 80$
Conv 1D	Filters = 16, Kernel Size = 3, ReLu	254 × 16
Batch Normalization	-	254 × 16
ReLu	-	254 × 16
Average Pooling	-	127 × 16
Dropout	0.2	127 × 16
Conv 1D	Filters = 4, Kernel Size = 3, ReLu	125 × 4
Batch Normalization	-	125 × 4
ReLu	-	125 × 4
Global Average Pooling	-	4
Batch Normalization	-	4
Dense	4 Units, Softmax	4

#### III. DATASET AND SIMULATION SETTINGS

All DL models used in this study were implemented into Google Colab, a free cloud-based platform that supports Python programming and offers virtual hardware, used for coding DL models. The dataset employed in the experimental study was generated using app Wireless Waveform Generator of MATLAB, which supports a wide range of waveform types, modulations, and wireless standards. Additionally, it allows to distort the waveform by adding different RF impairments. The tool also provides an option to export generated scripts for further customization (e.g., applying a fading channel model).

This study focuses on classifying data from distinct wireless standards with added impairments, a practical approach for scenarios like identifying unknown or jamming signals in a given RF channel. For this purpose, two standards were selected from each of the Wireless Personal Area Network (WPAN) and Wireless Local Area Network (WLAN) families: Bluetooth with Basic Rate/Enhanced Data Rate (BR/EDR) and ZigBee (IEEE 802.15.4) from WPAN, and IEEE 802.11b and IEEE 802.11ac from WLAN. The main parameters for packet generation for these standards are listed in Table IV and Table V, respectively. Other parameters available in the MATLAB function were kept at their default settings.

The waveform for each signal was generated as a single packet to ensure an accurate representation of the signal. In DL, maintaining balanced data representation is important. Due to the varying packet lengths among the generated signals, data truncation was implemented. Each packet was downsampled to  $2\times256$  I/Q data points. This size was selected to adequately represent each packet while avoiding excessive dataset enlargement, which could slow down the uploading and pre-processing phases. Each RF signal is represented by 1,500 packets for its respective SNR, varied across a range from  $-10\,\mathrm{dB}$  to  $20\,\mathrm{dB}$ .

A total of five datasets were generated: **Dataset no.1:** Each waveform in this dataset is influenced by Additive White Gaussian Noise (AWGN), phase offset, and I/Q-imbalance. The phase offset, randomly applied to each packet, was selected from the following values:  $10^{\circ}$ ,  $5^{\circ}$ ,  $0^{\circ}$ ,  $-5^{\circ}$ , and  $-10^{\circ}$ . Similarly, the I/Q-imbalance was applied with a random selection from values -10%, -5%, 0%, 5% and 10%.

TABLE IV: Parameters for WPAN packet generation

Parameter	Bluetooth BR/EDR	802.15.4 (ZigBee))
Mode	BR	-
Packet type	DM1 <sup>a</sup>	-
Payload Length	17 bytes	-
PSDU <sup>b</sup> Length	-	63 bytes
Modulation	GFSK	O-QPSK
Modulation index	0.3	-
Samples per chip	-	4
<sup>a</sup> Data Medium Rate, <sup>b</sup> Physical Layer Service Data Unit		

TABLE V: Parameters for WLAN packet generation

Parameter	IEEE 802.11b	IEEE 802.11ac
Transmission format	-	Very High Throughput (VHT)
Channel Bandwidth	20 MHz	80 MHz
MCSa	-	2 (QPSK)
Data rate	5.5 Mb/s	-
Modulation technique	DSSS <sup>b</sup>	OFDM <sup>c</sup>
PSDU Length	1000 bytes	1050 bytes

<sup>&</sup>lt;sup>a</sup>Modulation Coding Scheme, <sup>b</sup>Direct Sequence Spread Spectrum

Dataset no. 2: This dataset builds on the Dataset no. 1 by including Rician fading. The Rician channel model used in this work is emulated by six paths. The path delays range from 10 ns to 3700 ns, with no power loss in the first path (K = 10) [24] and gradually increasing to a 24 dB loss in the last path. The maximum Doppler shift is 50 Hz. Dataset no. 3: Similar to Dataset no. 2, this dataset uses Rayleigh fading channel instead of Rician. The parameters for the Rayleigh channel model are identical to the Rician channel, only K = 0. Dataset no.4: This dataset consists of only IEEE 802.11ac waveforms, each varying in their Modulation Coding Scheme (MCS). The MCS defines the coding and data rates as well as the underlying modulation. Waveforms are additionally influenced by phase offset, I/Q-imbalance, and AWGN. Dataset no.5: This dataset contains waveforms of different wireless standards, categorized as follows: a) IEEE 802.11n/ac with BPSK (MCS set to 0), b) IEEE 802.11ac with QPSK (MCS = 2), c) IEEE 802.11ac with 16-QAM (MCS = 4), and d) IEEE 802.11ac with 256-QAM (MCS =9). More systems parameters are provided in Table IV and Table V. All datasets are publicly available on GitHub [21].

## IV. RESULTS

The results were obtained using the test data, which comprised 15% of the total dataset. More precisely, 70% and 15% of the data were used to train and validate the DL-models, respectively. These processes were primarily executed on Google Colab, utilizing a free virtual T4 GPU, which provides significantly faster performance for DL-based algorithms compared to a standard CPU. All datasets had an input vector size  $2 \times 256$ . The accuracy of the DL models for each SNR value is shown in Figs. 4 and 5 while confusion matrices for all DL models at a specific SNR value are shown in Figs. 6-10.

As shown in Fig. 4(a), all the DL models studied achieve good accuracy in the classification of RF signals when these signals are influenced by the AWGN channel completed by phase offset and I/Q-imbalance. This is also reflected in the confusion matrices (see Fig. 6), which show promising classification accuracy SNR =  $2.6\,\mathrm{dB}$ .

<sup>&</sup>lt;sup>c</sup>Orthogonal Frequency Division Multiplexing

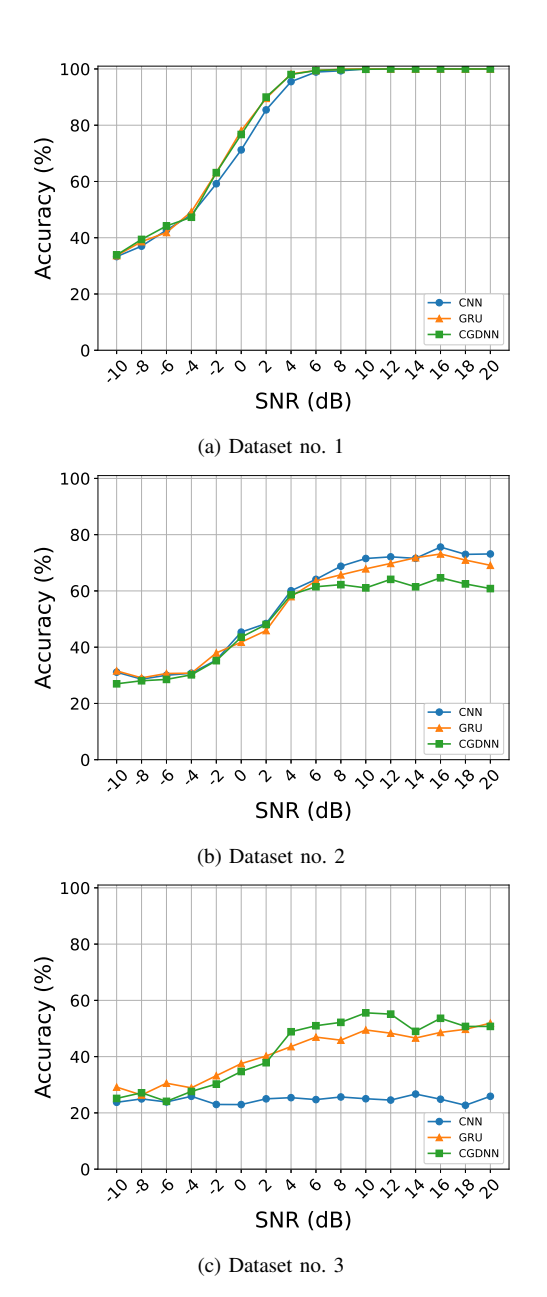


Fig. 4. Accuracy of DL models across all SNR values for Dataset no. 1-no. 3.

The primary challenge for all tested DL models lies in classifying ZigBee signal. However, for  $\rm SNR \geq 6\,dB$ , the DL models achieve nearly 100% classification accuracy.

Accuracy versus SNR for Dataset no. 3 and 4 containing waveforms among others influenced by Rician/Rayleigh fading channels are plotted in Figs. 4(b)-4(c), respectively. The results indicate limited accuracy across all DL models for fading channels. This is particularly evident for Rayleigh channel, where the CNN architecture has the poorest performance, achieving accuracy around 24% for all SNR values. Learning from sequences under the tested conditions, enabled by the RNN layers in CGDNN and GRU, appears to be more advantageous than relying predominantly on spatial data.

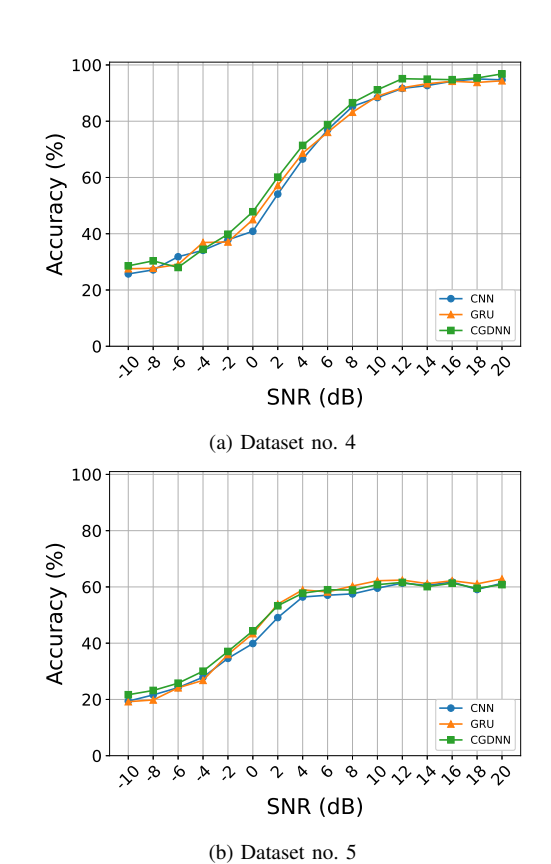


Fig. 5. Accuracy of DL models across all SNR values for Dataset no. 4 and no. 5.

Furthermore, the CGDNN achieves higher accuracy at lower SNR values compared to the GRU. Interestingly, for the Rician fading channel, the CNN outperforms the other models, achieving the best results under these conditions.

The results for the classification of IEEE 802.11ac waveforms with differing *MCS* are captured in Fig. 5 (a) and Fig. 9. Compared to the results for Dateset no. 1, see Fig. 4 (a), the classification accuracy of 802.11ac waveforms at lower SNR values is slightly worse. On the other hand, the increase in accuracy across higher SNR values in less step, stabilizing around 95%. Among the models, CGDNN has the best performance for this task. 16-QAM and 256-QAM digital modulations proved easier for the DL models to classify.

The classification accuracy of the DL models for Dataset no. 5, which contains the mixture of the waveforms of the generated RF signals, is shown Fig. 5(b) and Fig. 10. These signal waveforms were constructed by combining packets from the corresponding wireless standards under the same impairment conditions as in the previous datasets. The tested DL models showed limited accuracy in predicting mixed signals, such as Bluetooth + IEEE 802.11b and Bluetooth + IEEE 802.11ac, often favoring predictions of standalone signals or ZigBee mixed with 802.11b. This limitation stems from the dataset structure, where mixed signal packets often resembled those of independent signals, making classification ambiguous.

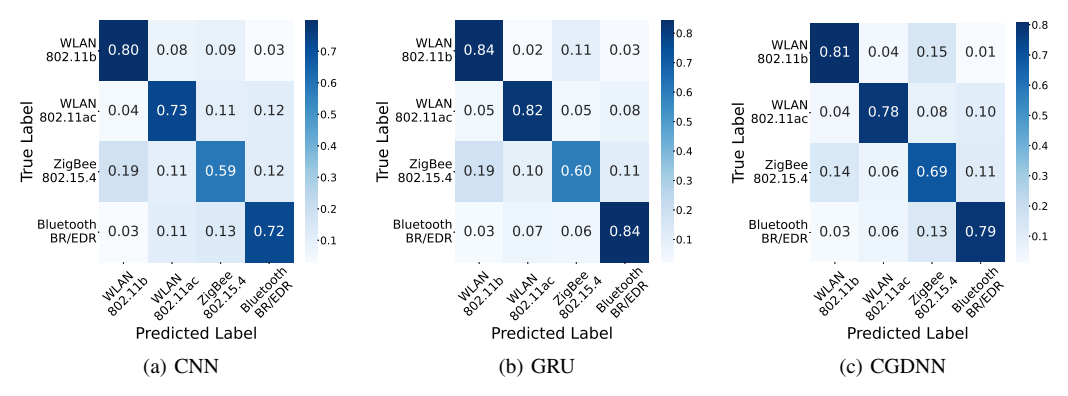


Fig. 6. Dataset no. 1: Confusion matrices for CNN, GRU, and CGDNN models at SNR = 0 dB.

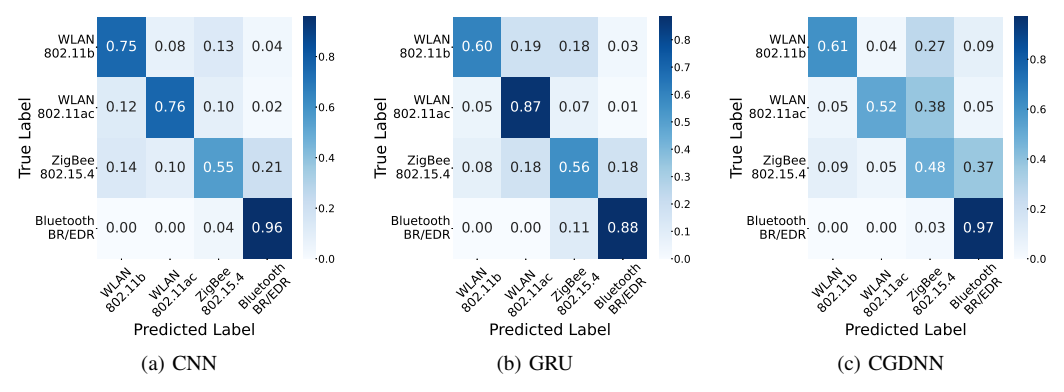


Fig. 7. Dataset no. 2: Confusion matrices for CNN, GRU, and CGDNN models at SNR = 16 dB.

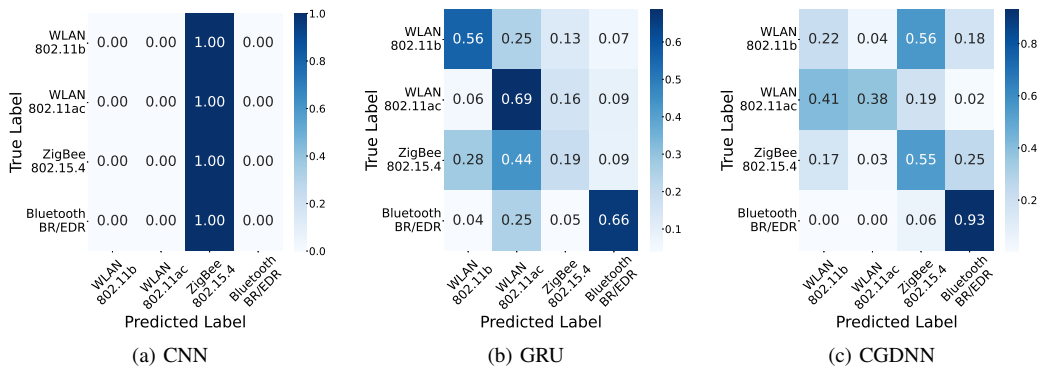


Fig. 8. Dataset no. 3: Confusion matrices for CNN, GRU, and CGDNN models at  $SNR = 20 \, dB$ .

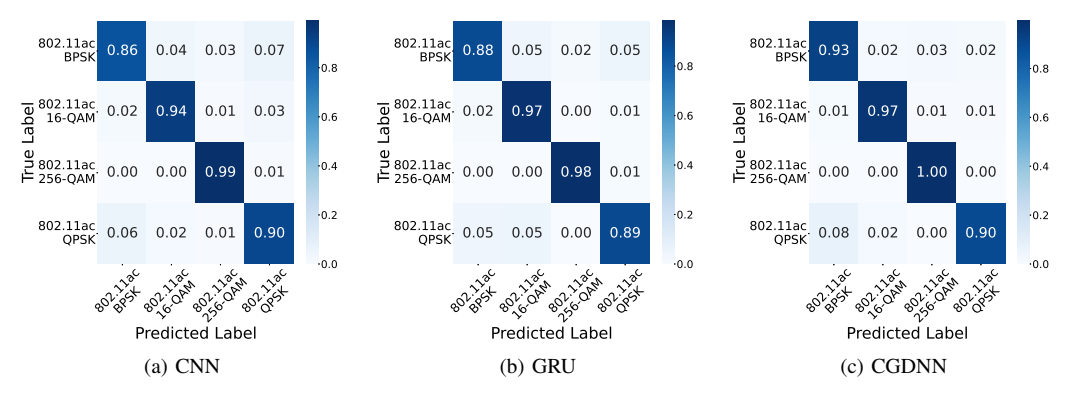


Fig. 9. Dataset no. 4: Confusion matrices for CNN, GRU, and CGDNN models at  $SNR = 14 \, dB$ .

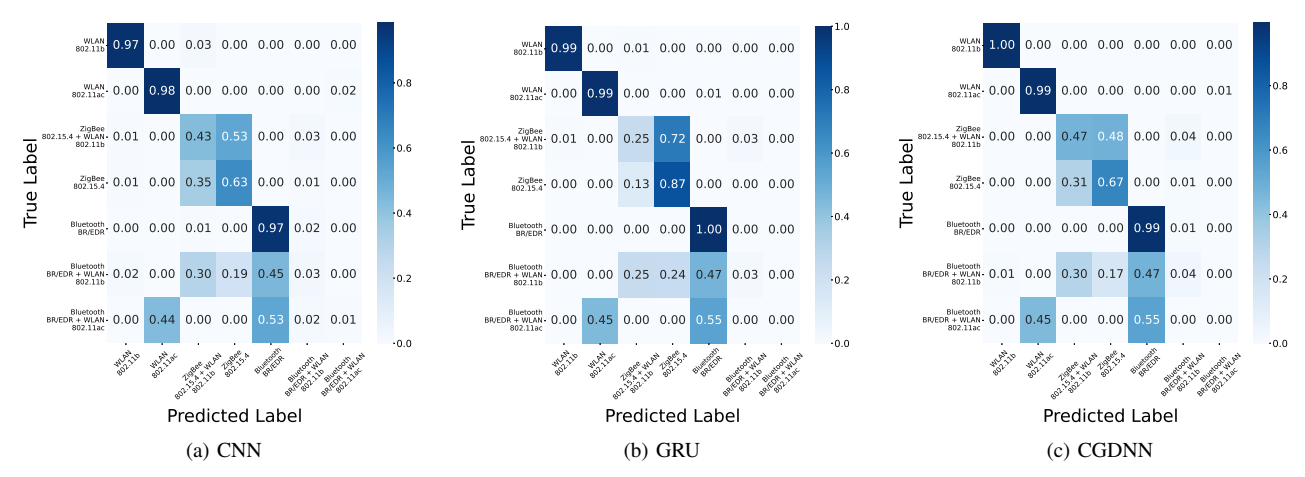


Fig. 10. Dataset no. 5: Confusion matrices for CNN, GRU, and CGDNN models at SNR = 6 dB.

While the DL models struggled to distinguish between mixed and individual signal classes, they successfully recognized ZigBee + 802.11b combinations as uniform ZigBee signals, suggesting pattern similarities between these classes.

#### V. CONCLUSION

This paper examined the classification of RF signals using DL-based approaches, specifically CNN, GRU, and CGDNN architectures. The results showed an increasing difficulty for each DL model to correctly classify the RF signals that are gradually influenced by impairments [25]. The CGDNN architecture provided the best results for most of the datasets. However, CNN performed best when Rician fading was considered, but it did not fit the data for Rayleigh fading. All results confirmed that further research in this area is very important. More details can be found in [21] and [22].

## REFERENCES

- T. S. Rappaport and et al., "Millimeter Wave Mobile Communications for 5G Cellular: It Will Work!" *IEEE Access*, vol. 1, pp. 335–349, 2013.
- [2] M. Simka and L. Polak, "On the RSSI-based Indoor Localization employing LoRa in the 2.4 GHz ISM Band," *Radioengineering*, vol. 31, no. 4, pp. 1–9, Apr. 2022.
- [3] L. Polak and et al., "Coexistence between DVB-T/T2 and LTE standards in common frequency bands," Wireless Personal Communications, vol. 88, pp. 669–684, 2016.
- [4] M. Banafaa and et al., "6G mobile communication technology: Requirements, targets, applications, challenges, advantages, and opportunities," Alexandria Engineering Journal, vol. 64, pp. 245–274, 2023.
- [5] M. Shahjalal and et al., "Enabling technologies for AI empowered 6G massive radio access networks," *ICT Express*, vol. 9, no. 3, pp. 341–355, 2023.
- [6] B. Velichkovska, A. Cholakoska, and V. Atanasovski, "Machine Learning Based Classification of IoT Traffic." *Radioengineering*, vol. 32, no. 2, pp. 256–263, 2023.
- [7] X. Liu, Y. Song, J. Zhu, F. Shu, and Y. Qian, "An Efficient Deep Learning Model for Generalized Automatic Modulation Recognition," *Radioengineering*, vol. 33, no. 4, pp. 713–720, Dec. 2024.
- [8] S. Peng, S. Sun, and Y.-D. Yao, "A Survey of Modulation Classification Using Deep Learning: Signal Representation and Data Preprocessing," *IEEE Trans. on Neural Networks and Learning Systems*, vol. 33, no. 12, pp. 7020–7038, 2022.
- [9] A. Jagannath, J. Jagannath, and P. S. P. V. Kumar, "A comprehensive survey on radio frequency (RF) fingerprinting: Traditional approaches, deep learning, and open challenges," *Computer Networks*, vol. 219, p. 109455, 2022.

- [10] K. Pijackova, "Radio modulation classification using deep learning architectures," June 2021, Bachelor's thesis. Brno: Brno University of Technology, Faculty of Electrical Engineering and Communication, Dept. of Radio Electronics.
- [11] M. Simic, M. Stankovic, and V. D. Orlic, "Automatic Modulation Classification of Real Signals in AWGN Channel Based on Sixth-Order Cumulants," *Radioengineering*, vol. 30, no. 1, 2021.
- [12] D. Hong, Z. Zhang, and X. Xu, "Automatic modulation classification using recurrent neural networks," in 2017 3rd IEEE Int. Conf. on Computer and Communications (ICCC), 2017, pp. 695–700.
- [13] A. P. Hermawan, R. R. Ginanjar, D.-S. Kim, and J.-M. Lee, "CNN-Based Automatic Modulation Classification for Beyond 5G Communications," *IEEE Communications Letters*, vol. 24, no. 5, pp. 1038–1041, 2020.
- [14] T. O'Shea and N. West, "Radio Machine Learning Dataset Generation with GNU Radio," *Proceedings of the GNU Radio Conference*, vol. 1, no. 1, 2016.
- [15] P. Hu, W. Yang, N. Pu, Y. Peng, and X. Ding, "A New Deep Architecture for Digital Signal Modulation Classification over Rician Fading," in 2021 IEEE 6th Int. Conf. ICCCS, 2021, pp. 856–860.
- [16] Y. Shi, K. Davaslioglu, Y. E. Sagduyu, W. C. Headley, M. Fowler, and G. Green, "Deep Learning for RF Signal Classification in Unknown and Dynamic Spectrum Environments," in 2019 IEEE Int. Symp. on Dynamic Spectrum Access Networks (DySPAN), 2019, pp. 1–10.
- [17] Z. Chen and et al., "SigNet: A Novel Deep Learning Framework for Radio Signal Classification," *IEEE Transactions on Cognitive Commu*nications and Networking, vol. 8, no. 2, pp. 529–541, 2022.
- [18] A. Olesiński and Z. Piotrowski, "A Radio Frequency Region-of-Interest Convolutional Neural Network for Wideband Spectrum Sensing," Sensors, vol. 23, no. 14, p. 6480, 2023.
- [19] R. D. Badger, K. H. Jung, and M. Kim, "An Open-Sourced Time-Frequency Domain RF Classification Framework," in 2021 29th European Signal Processing Conference (EUSIPCO), 2021, pp. 1701–1705.
- [20] W. Zhang, M. Feng, M. Krunz, and A. Hossein Yazdani Abyaneh, "Signal Detection and Classification in Shared Spectrum: A Deep Learning Approach," in *IEEE INFOCOM 2021 - IEEE Conference on Computer Communications*, 2021, pp. 1–10.
- [21] S. Turak, "GitHub: AI-based classification of RF signals," June 2024. [Online]. Available: https://github.com/Samuelturak/Master-s-thesis
- [22] ——, "AI-based classification of RF signals," June 2024, Master's thesis. Brno: Brno University of Technology, Faculty of Electrical Engineering and Communication, Department of Radio Electronics.
- [23] N. Kassri and et al., "Pruning-based Hybrid Neural Network for Automatic Moudlation Calssification in Cognitive Radio Networks," J. of Theo. and Appl. Inform. Technology, vol. 102, no. 3, pp. 898–913, 2024.
- Theo. and Appl. Inform. Technology, vol. 102, no. 3, pp. 898–913, 2024.
  [24] D. Du, X. Zeng, X. Jian, F. Yu, and L. Miao, "Analysis of Three-Dimensional Spatial Selectivity for Rician Channel," *Radioengineering*, vol. 27, no. 1, pp. 249–255, 2018.
- [25] K. Tamizhelakkiya, S. Gauni, and P. Chandhar, "Transfer Learning Based Location-Aided Modulation Classification in Indoor Environments for Cognitive Radio Applications," *Radioengineering*, vol. 32, no. 4, 2023.